applied sciences

MDPI

Technical Note

Measurement of Unit Weight of Dry Sand Using Piezoelectric Sensor

Sung-Sik Park [1], Jung-Shin Lee [1], Dong-Eun Lee [2] and Jun-Cheol Lee [3,*]

[1] Department of Civil Engineering, Kyungpook National University, 80 Daehakro, Bukgu, Daegu 41566, Korea; sungpark@knu.ac.kr (S.-S.P.); jhjs14@knu.ac.kr (J.-S.L.)
[2] School of Architecture and Civil Engineering, Kyungpook National University, 80 Daehakro, Bukgu, Daegu 41566, Korea; dolee@knu.ac.kr
[3] Daegyeong Regional Infrastructure Technology Development Center, Kyungpook National University, 80 Daehakro, Bukgu, Daegu 41566, Korea
* Correspondence: darkgreen@knu.ac.kr; Tel.: +82-53-950-6335

Received: 16 October 2018; Accepted: 14 November 2018; Published: 18 November 2018

Abstract: Recently, an electro-mechanical impedance (EMI) technique has found wide application in the monitoring of concrete structures. This EMI technique was employed for measuring the unit weights of various grain sizes of sand and the relevant process is reported herein. A piezoelectric sensor (PZT, i.e., lead zirconate titanate sensor) was imbedded into small, medium, and large-sized grains of the Nakdong river sand and a surcharge was applied. The effect of an increase in unit weight owing to the surcharge was investigated in terms of the resonant frequency (peak frequency) and corresponding conductance at resonant frequency (peak conductance). A ceramic-coated PZT sensor was used to prevent the occurrence of a short circuit. The measured peak frequency and conductance from the PZT sensor were correlated with the unit weight of sand. With an increase in the unit weight of sand, the peak PZT frequency was found to have increased, however, the peak conductance was seen to have decreased. The peak PZT frequency and conductance were seen to be strongly correlated with the unit weight of Nakdong river sand except for the peak conductance of large grain sized sand.

Keywords: electro-mechanical impedance; piezoelectric; frequency; conductance; unit weight; sand

1. Introduction

Piezoelectric materials (PZT, i.e., lead zirconate titanate) often find varied applications in civil engineering projects. One of the PZT sensors, called the bender element, has been used to generate shear or compressive waves during laboratory testing [1–4]. On the other hand, the electro-mechanical impedance (EMI) technique employing PZT sensors has been widely used as a non-destructive testing technique for monitoring concrete structures. When using this technique, the PZT material is usually attached to the surface of concrete and steel bridges and other such concrete structures to monitor their strength or deformation [5–7]. Recently, the technique was used to measure the curing conditions of concrete [8–10].

Soil compaction is the most fundamental procedure in soil engineering. The degree of soil compaction can be determined by measuring the unit weight (density) of compacted soils. Three methods are usually used to determine the in situ density of compacted soils: (a) The sand-cone method; (b) the rubber-balloon method; and (c) the nuclear method. Soil densities around pipes or retaining walls could be reduced owing to soil washing due to leakage or groundwater flow [11]. At times, cavitation may also occur resulting in ground subduction. Recently, many instances of ground failure caused by such changes in soil density have been noticed. The three methods for

determining the in situ density are not able to measure the continuous variation of density. It has, therefore, become necessary to regularly monitor the unit weight of soils in the field.

In this study, a PZT sensor was embedded in three different grain sizes (small, medium, and large) of the Nakdong river sand. The sand grains were poured into the small compaction mold and four different levels of surcharge were applied on the surface of each type of sand. Subsequently, the frequency and conductance of the PZT sensor were measured for each type of sand under the different levels of load. The resonant frequency and corresponding conductance of the PZT sensor in a specific frequency range were then correlated with the level of load and corresponding unit weight or density of sand. Such a relationship could be used to predict the unit weight of soil subjected to compaction, loosening, or cavitation in the field.

2. Piezoelectric Sensor and Sample Preparation

A picture of the PZT sensor used in this study is shown in Figure 1a. Dimensions of the PZT sensor are indicated in the schematic shown in Figure 1b. When the PZT senor embeds in soil, it faces the risk of short circuiting due to moisture in the soil. In this study, the sensor was coated with a ceramic to prevent the event of a short circuit. Figure 2 shows the EMI signature of uncoated and ceramic coated PZT sensors immersed in 10% $CaCl_2$ solution. As seen in Figure 2, the EMI signature of the PZT senor showed the double resonance peaks in the frequency range of 50 to 350 kHz. In this study, the behavior of the EMI signature was analyzed using the peak corresponding to the frequency of 130 kHz under free vibration in air condition.

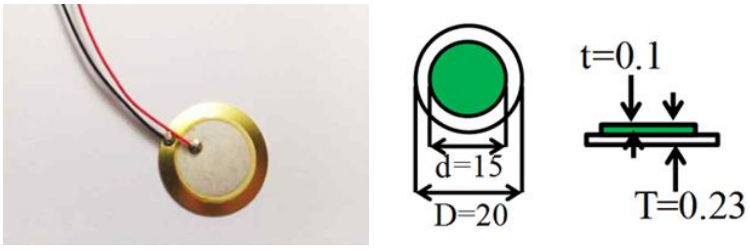

(**a**) (**b**)

Figure 1. Piezoelectric sensor (PZT) after coating and its dimensions (unit: mm): (**a**) PZT sensor used in this study; (**b**) dimensions of the PZT patch.

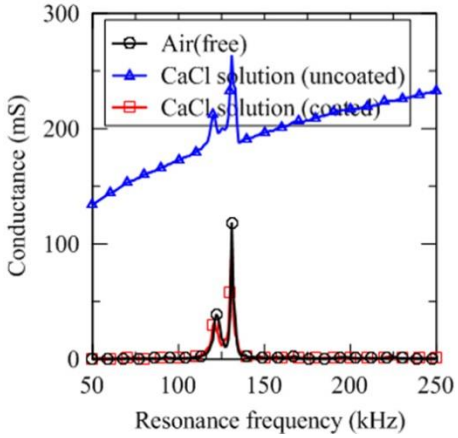

Figure 2. Electro-mechanical impedance (EMI) signatures of PZT sensor under various conditions.

The EMI signature of the immersed, uncoated PZT sensor was very different from that of the PZT sensor under the free vibration in air condition. In the case of the EMI signatures of the coated PZT sensor immersed in $CaCl_2$ solution compared with that in free vibration in air condition, the EMI peak magnitudes were slightly different but the EMI peak frequencies were the same. The difference in EMI

peak magnitude was caused by the difference of the surrounding material of the PZT sensor. This means that a short circuit was avoided, and EMI sensing was possible even with moisture in the soil.

Figure 3 shows the EMI signatures of the PZT sensor coated with ceramic under various temperature conditions. As shown in Figure 4, the EMI peak magnitudes were increased slightly with the increase of the temperature, but the EMI peak frequencies were not changed significantly. It can be seen that the increase of EMI peak magnitude with the increase of temperature is probably due to the thermal stress in the PZT sensor. Since the change of EMI signature by temperature was very small compared with the change of EMI signature in the soil experiment, the effect of temperature can be ignored in this study.

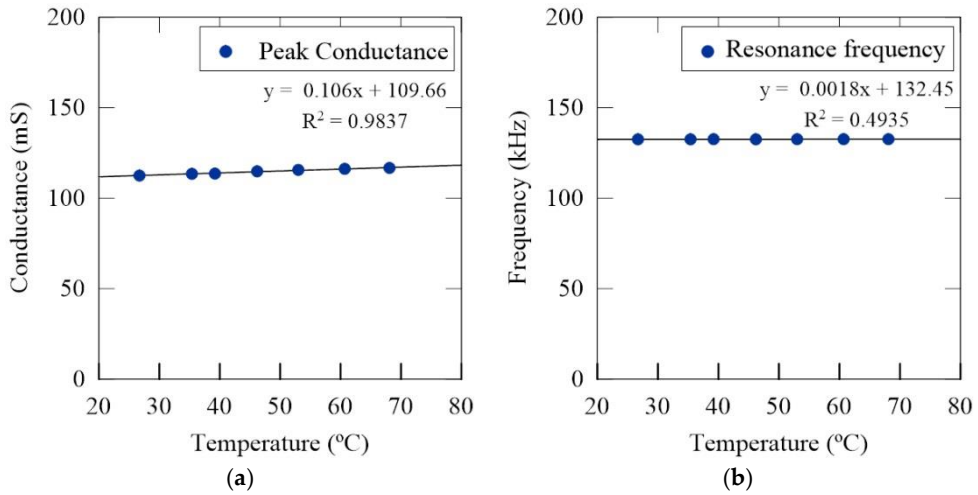

Figure 3. The changes of EMI signatures with the increase of temperature: (**a**) Relationship between temperature and resonance peak magnitude; (**b**) relationship between temperature and EMI peak frequency at resonance peak.

The EMI measuring system employed in this study, as depicted in Figure 4, comprises an LCR meter, PZT sensor, GP-IB interface, and software. The PZT sensor, without being placed in the soil, demonstrated three modes of resonant frequencies (130, 468, and 662 kHz) below 1 MHz. It seems that the vibration occurs in multiple directions because of the circular shape of the PZT sensor. The frequency range of 50–350 kHz (500 Hz intervals) within the first mode of resonance was selected for use in this study to easily distinguish between different soil densities.

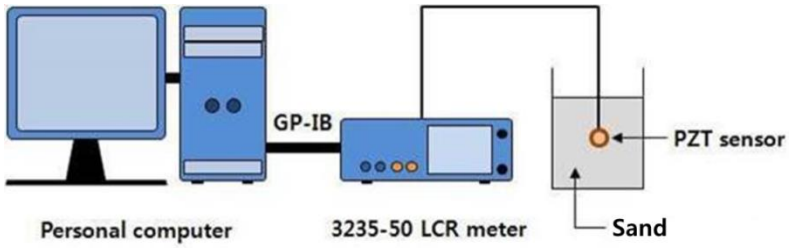

Figure 4. EMI measurement system using PZT sensor.

The series of EMI sensing experiments for different levels of surcharge were performed on the Nakdong river sand. The sand was dried and sieved into three different grain sizes—small (0.075–0.85 mm), medium (0.85–2.0 mm), and large (2.0–4.75 mm)—as shown in Figure 5a. Grain size distribution curves and properties of the three sand types are compared in Figure 5b and Table 1. The specific gravity of each grain size was constant at 2.65. The sand was loosely poured into a compaction mold measuring 15 cm in diameter and 17 cm in height as shown in Figure 6. The PZT sensor was located at the center of the mold, and, subsequently, four levels of surcharge were applied

on the surface of sand. Ratios of the diameter of the PZT sensor (DPZT) to the mean grain size of sand (D50) were of the order of 47, 17, and 6 for the small, medium, and large-sized sand grains respectively.

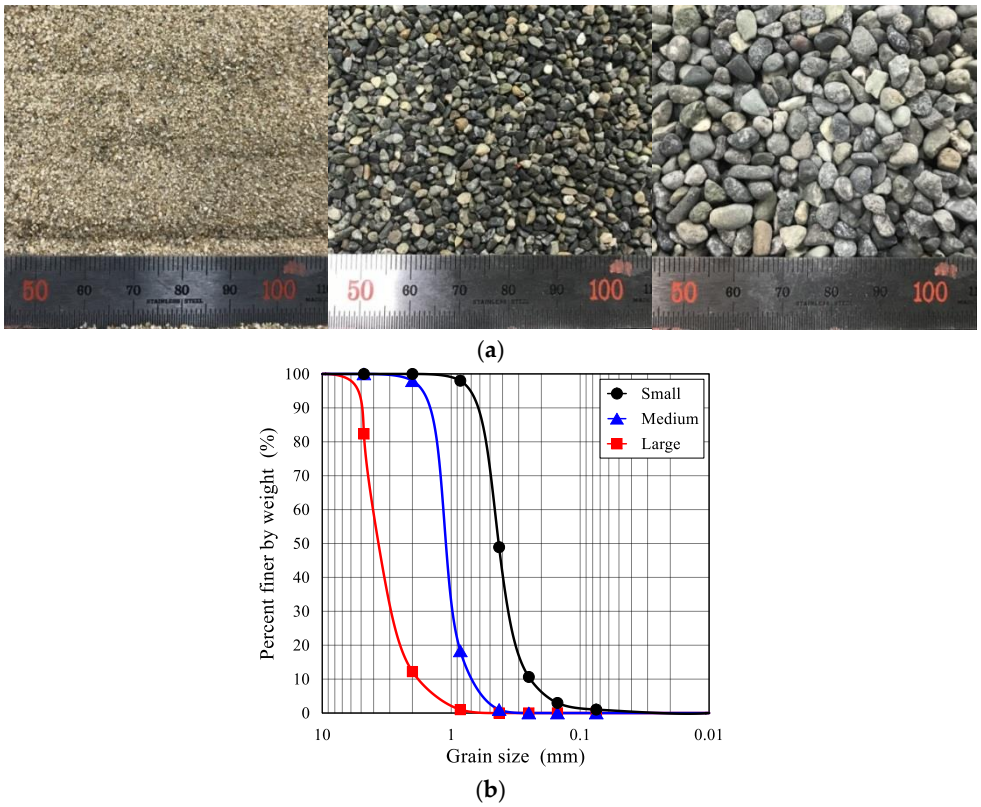

Figure 5. Nakdong river sand: (**a**) Pictures of small, medium, and large-sized sands; (**b**) grain size distribution curves.

Table 1. Material properties of Nakdong river sand.

Size	D60 [(i)] (mm)	D30 [(ii)] (mm)	D10 [(iii)] (mm)	Coef. of Uniformity, Cu	Coef. of Curvature, Cg	Unified Soil Classification System	DPZT/D50
Small	0.62	0.31	0.053	0.830	0.28	SP [(iv)]	47
Medium	2.62	2.46	2.16	1.98	1.34	SP	17
Large	4.25	4.04	3.66	3.02	1.04	SP	6

Note: (i) D60 is a diameter corresponding to 60% finer; (ii) D30 is a diameter corresponding to 30% finer; (iii) D10 is a diameter corresponding to 10% finer; (iv) SP is a poorly graded sand.

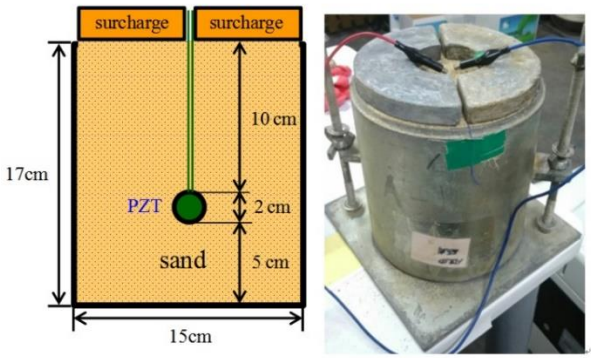

Figure 6. Experimental setup for EMI measurement.

3. Results of EMI Sensing

Table 2 summarizes all testing cases for the three sand types in terms of the resonant frequency (peak frequency) and the corresponding value of conductance at resonant frequency (peak conductance). The initial dry unit weights of the three sand types were determined to be 14.45, 15.74, and 16.83 kN/m^3 without surcharge. The unit weights of sand after application of different surcharge levels were determined via consideration of the settled surface. The calculated dry unit weights of the three sand types are compared in Table 2 and shown in Figure 7. With an increase in surcharge levels, the unit weight of sand was found to have gradually increased. The variation in unit weight was most dominant for small-sized sand grains, its value ranging from 14.45–17.49 kN/m^{3-} as shown in Figure 5.

Table 2. Results of EMI sensing.

Cases	Small Sand			Medium Sand			Large Sand		
	Unit Weight (kN/m^3)	Peak Frequency (kHz)	Peak Conductance (S)	Unit Weight (kN/m^3)	Peak Frequency (kHz)	Peak Conductance (S)	Unit Weight (kN/m^3)	Peak Frequency (kHz)	Peak Conductance (S)
Sand	14.45	172.0	0.06	15.74	175.7	0.09	16.83	173.2	0.08
Sand + 6 kPa	16.09	173.9	0.04	16.32	176.3	0.08	17.34	173.7	0.08
Sand + 11 kPa	16.65	174.9	0.02	16.52	176.7	0.07	17.44	174.2	0.08
Sand + 17 kPa	17.24	176.1	0.02	16.62	177.0	0.07	17.55	174.3	0.07
Sand + 23 kPa	17.49	177.0	0.01	16.93	178.0	0.06	17.66	174.5	0.08

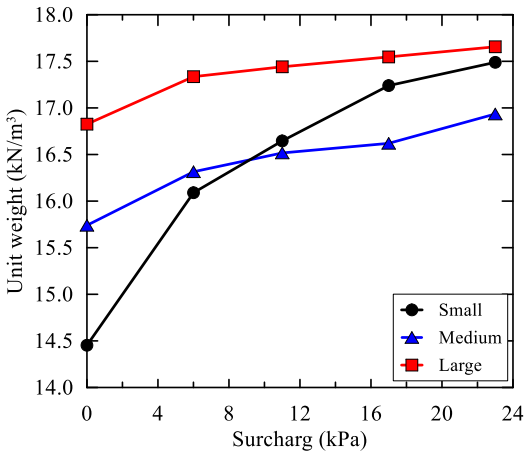

Figure 7. Relationship between surcharge and unit weight for three sand types.

3.1. Effect of Surcharge on EMI Sensing

The effects of the surcharge application during EMI sensing experiments were investigated in terms of peak frequency and corresponding peak conductance. Figure 6 demonstrates the relationship between conductance and frequency for the three sand grain sizes. With an increase in surcharge levels on sand, the peak frequency was found to have gradually increased across all sand grain sizes. This result may be attributed to increased sand stiffness due to the increase in unit weight caused by the application of surcharge, as shown in Figure 8. Consequently, vibrations in the sand were reduced and the peak frequency increased. The peak conductance, on the other hand, demonstrated a slight decrease with an increase in surcharge levels. Lee et al. (2015) [12] demonstrated a similar increase in peak frequency and decrease in peak conductance corresponding to an increase in hardness of mortar.

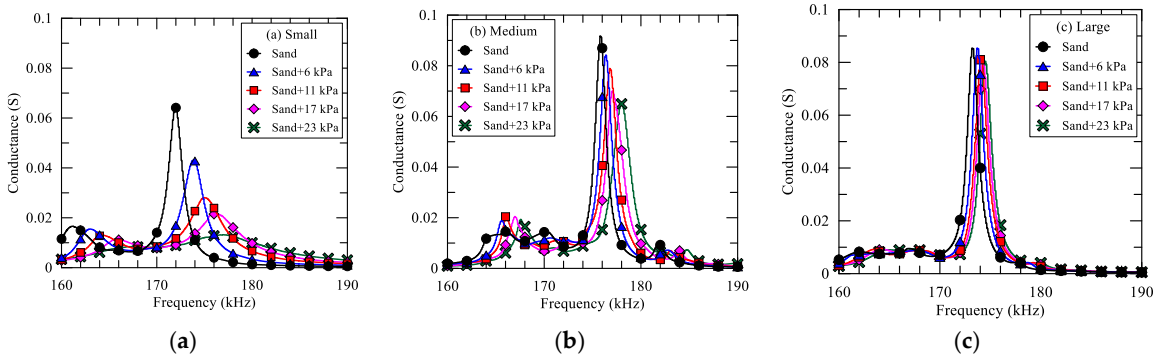

Figure 8. Conductance versus frequency for three sand types: (**a**) Signatures of EMI for the small-sized sand; (**b**) signatures of EMI for the medium-sized sand; (**c**) signatures of EMI for the large-sized sand.

Soils in the field comprise various grain sizes and, therefore, three different grain sizes of sand were used in the EMI sensing experiment. Figure 9 compares the values of the peak frequency and the peak conductance for the three sand grain sizes. The effect of an increase in the unit weight corresponding to an increase in surcharge levels was found to be most noticeable in the sand comprising small-sized sand grains. For medium and large-sized sand grains, the effect was not prominent. This result seems to be related to the contact area between sand grains and the PZT sensor. The relative size of sand particles compared to the PZT sensor could have an influence on the frequency and conductance. For example, the ratio of the diameter of the PZT sensor to mean grain size of the large and medium-sized sand grains (DPZT/D50) was 6 and 17, respectively. Compared to small-sized sand grains (DPZT/D50 = 47), such large grain sizes of sand are unlikely to effect a large change in the results obtained via EMI sensing.

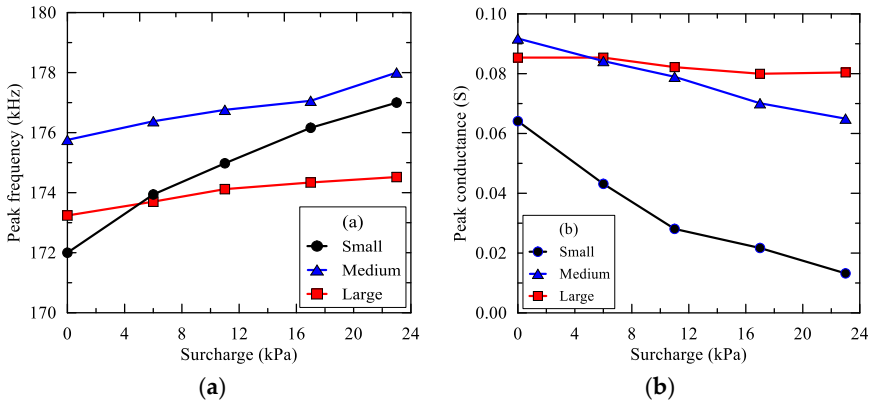

Figure 9. Effect of surcharge on peak frequency and conductance for three sand types: (**a**) Peak frequency–surcharge curve; (**b**) peak conductance–surcharge curve.

3.2. Relationship between Unit Weight and Frequency and Conductance

Table 2 summarizes the results of unit weight change caused by an increase in surcharge levels. As shown in Figure 10, the peak frequency demonstrated an increase although the decrease in peak conductance was observed with an increase in surcharge levels regardless of the sand size. This effect was most dominant for the small-sized Nakdong river sand.

For the medium and large-sized sand grains used in this study, changes in peak frequency and conductance were small when the different levels of surcharge were applied on top of the specimen. This is because the amount of surcharge itself was low and the transferred load to sand particles was also small. This resulted in only a small change in the unit weight, which had a marginal influence on the measured frequency and conductance of the 20 mm PZT sensor.

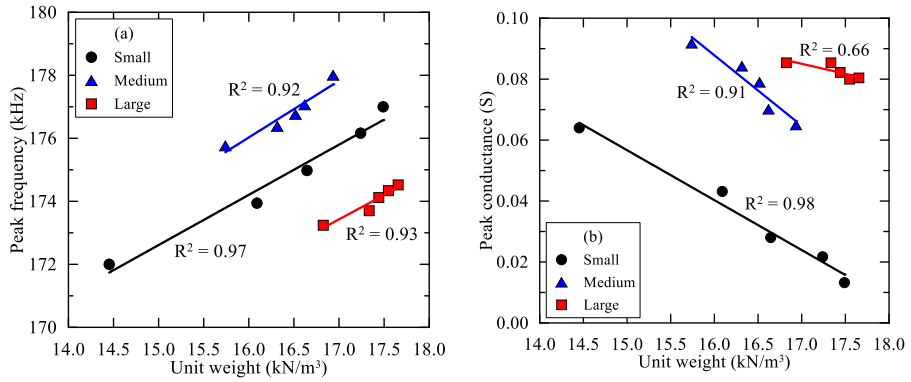

Figure 10. Effect of unit weight increase on peak frequency and conductance for three sand types: (**a**) Relationship between the peak frequency and the unit weight; (**b**) relationship between the peak conductance and the unit weight.

4. Discussion

In this study, the unit weight of sand with three different particle sizes was evaluated by an EMI sensing technique. The EMI peak magnitude was decreased with the increase of surcharge on sand. At the same time, the EMI peak frequency shifted toward a higher frequency domain with the increase of surcharge on sand.

As the sand became stiffer due to unit weight increase caused by surcharge, the vibration of the PZT sensor became less and the peak frequency increased. This relationship was most dominant for the small grain sized Nakdong river sand. As a key finding of this study, the relationship between the dry unit weight (r_d) and the peak frequency (f_0) for the small Nakdong river sand was derived from Equation (1) from Figure 8a. As shown in the figure, as unit weight increased, the peak frequency increased and the peak conductance decreased. By using this kind of result, we can predict the variation of unit weight in the field due to compaction or surcharge loading according to

$$f_0\ (\text{kHz}) = 1.593 \times r_d\ (\text{kN/m}^3) + 148.71. \quad (1)$$

In the previous studies using EMI sensing techniques, the EMI signatures were analyzed with converting data, i.e., RMSD (root mean square deviation) and Mahalanobis distance, because the variation of EMI signatures was very small [13,14]. However, in this study the clear changes in EMI signatures were found and the unit weight of soil was evaluated using only the EMI signatures, without the conversion of data. Therefore, it can be concluded that the unit weight of soil can be effectively monitored through the changes of EMI signatures.

5. Conclusions

Three grain sizes of the clean Nakdong river sand were poured into a small compaction mold and subsequently applied with surcharge. The series of EMI sensing experiments were performed on the three different grain sizes of sands. Four levels of surcharge (6, 11, 17, 23 kPa) were applied to the surface of the sand. The results were compared in terms of the peak frequency and conductance and may be listed as follows:

(1) With an increase in surcharge levels, the peak frequency demonstrated the corresponding increase, but the peak conductance was found to decrease.
(2) The unit weight of the sand demonstrated a strong correlation with the measured peak frequency and conductance, except for the peak conductance of large grain sized sand.
(3) The relationship between the peak frequency or conductance and unit weight of sand could be found useful in predicting the degree of soil compaction, loosening, or cavitation in the field.

Author Contributions: Conceptualization, S.-S.P. and J.-C.L.; methodology, J.-S.L. and D.-E.L.; formal analysis, S.-S.P. and J.-C.L.; writing original draft preparation, J.-S.L.; writing review and editing, S.-S.P. and J.-C.L.; supervision, S.-S.P.

Funding: This work was supported by the National Research Foundation of Korea (NRF) grant funded by the Korea government (No. NRF-2018R1A5A1025137).

Conflicts of Interest: The authors declare no conflict of interest.

References

1. Dyvik, R.; Madshus, C. Laboratory Measurement of Gmax Using Bender Elements. In Proceedings of the ASCE Annual Convention, Advances in the Art of Testing Soil Under Cyclic Conditions, Detroit, MI, USA, 24 Januray 1986.
2. Lee, J.S.; Lee, C.H. Principles and Considerations of Bender Element Tests. *J. Korean Geotech. Soc.* **2006**, *22*, 47–57.
3. Shirley, D.J.; Hampton, L.D. Shear wave measurements in laboratory sediments. *J. Acoust. Soc. Am.* **1978**, *63*, 607–613. [CrossRef]
4. Suwal, L.P.; Kuwano, R. Disk shaped piezo-ceramic transducer for P and S wave measurement in a laboratory soil specimen. *Soils Found.* **2013**, *53*, 510–524. [CrossRef]
5. Park, G.; Cudney, H.H.; Inman, D.J. Impedance-Based Health Monitoring of Civil Structural Components. *J. Infrastruct. Syst.* **2000**, *6*, 153–160. [CrossRef]
6. Ayres, J.W.; Lalande, F.; Chaudhry, Z.; Rogers, C.A. Qualitative Impedance-Based Health Monitoring of Civil Infrastructures. *Smart Mater. Struct.* **1998**, *7*, 599–605. [CrossRef]
7. Soh, C.K.; Tseng, K.K.H.; Bhalla, S.; Gupta, A. Performance of Smart Piezoceramic Patches in Health Monitoring of a RC Bridge. *Smart Mater. Struct.* **2000**, *9*, 533–542. [CrossRef]
8. Lee, C.J.; Lee, J.C.; Shin, S.W.; Kim, W.J. Investigation of setting process of cementitious materials using electromechanical impedance of embedded piezoelectric path. *J. Korea Inst. Build. Constr.* **2012**, *12*, 607–614. [CrossRef]
9. Gu, H.; Song, G.; Dhonde, H.; Mo, Y.L.; Yan, S. Concrete early-age strength monitoring using embedded piezoelectric transducers. *Smart Mater. Struct.* **2006**, *15*, 1837–1845. [CrossRef]
10. Wang, D.; Zhu, H. Monitoring of the strength gain of concrete using embedded PZT impedance transducer. *Constr. Build. Mater.* **2011**, *25*, 3703–3708. [CrossRef]
11. Das, B.M. *Principles of Geotechnical Engineering*, 7th ed.; Cengage Learning: Boston, MA, USA, 2009; p. 137. ISBN 978-0-49-541130-7.
12. Lee, J.C.; Shin, S.W.; Kim, W.J.; Lee, C.J. Electro-mechanical impedance based monitoring for the setting of cement paste using piezoelectricity sensor. *Smart Struct. Syst.* **2016**, *17*, 123–134. [CrossRef]
13. Silva, R.N.F.; Tsuruta, K.M.; Rabelo, D.S.; Finzi, R.M.; Steffen, V. The use of electromechanical impedance based structural health monitoring technique in concrete structure. In Proceedings of the 8th European Workshop on Structural Health Monitoring, Bilbao, Spain, 5–8 July 2016.
14. Wang, D.; Wang, Q.; Wang, H.; Zhu, H. Experimental study on damage detection in timber specimens based on an electromechanical impedance technique and RMSD-based mahalanobis distance. *Sensors* **2016**, *16*, 1765. [CrossRef] [PubMed]